

Effects of gomisin A on vascular contraction in rat aortic rings

| | |
|-------|---|
| メタデータ | 言語: eng 出版者: 公開日: 2017-10-03 キーワード (Ja): キーワード (En): 作成者: メールアドレス: 所属: |
| URL | http://hdl.handle.net/2297/26244 |

Effects of gomisin A on vascular contraction in rat aortic rings

Young Mi Seok^{1#}, Young Whan Choi^{2#}, Gyung-Duck Kim³, Hye Young Kim⁴, Yoh Takuwa⁵
and In Kyeom Kim^{1,4*}

¹Cardiovascular Research Institute, ⁴Department of Pharmacology, Kyungpook National University School of Medicine, Daegu, 700-422, Republic of Korea

²Department of Horticultural Bioscience, Pusan National University, Miryang 627-706, Republic of Korea

³Department of Nursing, Daegu Health College, Daegu 702-722, Republic of Korea

⁵Department of Physiology, Kanazawa University Graduate School of Medicine, 13-1 Takara-machi, Kanazawa, Ishikawa 920-8640, Japan.

These authors equally contributed to this paper.

*Correspondence and Proofs

In Kyeom Kim, M.D., Ph.D.

Department of Pharmacology

Kyungpook National University School of Medicine

Daegu, 700-422, Republic of Korea

Tel: +82-53-420-4833 Fax: +82-53-426-7345

E-mail: inkim@knu.ac.kr

Abstract

Gomisin A (GA) is an active ingredient of the fruits of *Schisandra chinensis* which has been widely used as a tonic in traditional Korean medicine. GA induces not only endothelium-dependent but also endothelium-independent relaxation in isolated rat thoracic aorta. This study was aimed to investigate the molecular mechanism by which GA induces endothelium-independent vasorelaxation. Rat aortic rings were denuded of endothelium, mounted in organ baths, and subjected to contraction or relaxation. We measured the amount of GTP RhoA as well as the phosphorylation level of 20 kDa myosin light chains (MLC₂₀), myosin phosphatase targeting subunit 1 (MYPT1) and protein kinase C (PKC)-potentiated inhibitory protein for heterotrimeric myosin light chain phosphatase (MLCP) of 17kDa (CPI17). Pretreatment with GA dose-dependently inhibited the concentration-response curves in response to sodium fluoride (NaF) or thromboxane A₂ agonist U46619, but not to phorbol 12, 13-dibutyrate (PDBu). GA decreased the activation of RhoA as well as the phosphorylation level of MLC₂₀, MYPT1_{Thr855} and CPI17 induced by 8.0 mM NaF or 30 nM U46619. However, K⁺ channel blockers such as glibenclamide (GB), apamin (Apa), or charybdotoxin (CTX) did not affect the vascular relaxation induced by GA. Furthermore, GA did not affect the level of phosphorylation of CPI17 induced by PDBu. GA reduces vascular contraction through inhibition of RhoA/Rho-kinase pathway in endothelium-denuded rat aorta.

Key words gomisin A · RhoA/Rho-kinase · vasorelaxation · MYPT1 · CPI17 · K⁺ channel blocker

Abbreviation

GA, Gomisin A;

MLC₂₀, 20 kDa myosin light chains;

MLCP, myosin light chain phosphatase;

MYPT1, myosin phosphatase targeting subunit 1;

CPI17, PKC-potentiated inhibitory protein for heterotrimeric MLCP of 17kDa;

NaF, sodium fluoride;

PDBu, phorbol 12, 13-dibutyrate;

PKC, protein kinase C;

GB, glibenclamide;

Apa, apamin;

CTX, charybdotoxin;

Acknowledgments

This work was supported by the National Research Foundation of Korea Grant funded by the Korean Government [NRF-2009-353-E00024], [NRF-2010-616-E00004] and the Brain Korea 21 Project in 2010.

Introduction

Gomisin A (GA) is a small molecular weight lignan contained in Fructus Schisandrae, the dried seed of *Schisandra chinensis* which is widely used as a health food product and a tonic in traditional Korean medicine (Park et al. 2007). *Schisandra chinensis* have some beneficial effects including hepatoprotective, antioxidative, anti-inflammatory, anticancer, and anti-HIV actions (Chen et al. 1997; Chiu et al. 2002; Choi et al. 2006; Wu et al. 2003; Yasukawa et al. 1992). The fruit of *Schisandra chinensis* is known to be enriched with lignans (Nakajima et al. 1983), of which schisandrin (2-9%), γ -schisandrin (1-5%), deoxyschisandrin (0.2-1.1%), and GA (0.7-3%) are major ingredients, depending on the plant origin and harvest season (% dry weight) (He et al. 1997; Park et al. 2007).

GA or an aqueous extract of *Schisandra chinensis* induced not only endothelium-dependent but also endothelium-independent vascular relaxation in isolated thoracic aorta through activation of nitric oxide (NO) pathway in endothelium or direct dephosphorylation of MLC in vascular smooth muscle (Park et al. 2007; Rhyu et al. 2006). GA releases nitric oxide from endothelium through Ca^{2+} -dependent activation and translocation of eNOS (Park et al. 2009a). Moreover, the relaxation by GA in endothelium-denuded aortic rings were inhibited by calyculin, an inhibitor of MLC phosphatase, implicating involvement of RhoA/Rho-kinase signaling pathway which inhibits MLC phosphatase. The small GTPase RhoA plays an important role as a molecular switch in the enhancement of Ca^{2+} sensitivity of smooth muscle contraction (Hirata et al. 1992). The activation of RhoA leads to the subsequent activation of an effector, Rho-kinase (Leung et al. 1995). Activation of Rho-kinase decreases the activity of myosin light chain phosphatase (MLCP) through phosphorylation of MYPT1 at Thr855 and CPI17 at Thr38, resulting in enhancement of vascular contractility (Somlyo et al. 2003). The RhoA/Rho-kinase plays an important role in development of cardiovascular diseases such as heart failure, coronary artery disease,

pulmonary hypertension, arteriosclerosis, restenosis, and stroke which show excessive activation of the RhoA/Rho-kinase signaling pathway (Budzyn et al. 2006; Budzyn et al. 2007; Hirooka et al. 2004; Shimokawa et al. 2005). Recently the RhoA/Rho kinase pathway has received attention as genetic disruption of the pathway blocks elevation of vascular tone under hypertensive condition without affecting regulation of the blood pressure (Wirth et al. 2008).

Here we investigated the mechanism by which GA inhibits vascular smooth muscle contraction. Therefore, the purpose of present study was to investigate the inhibitory effects of GA on RhoA activation and subsequent phosphorylation of MYPT1 or CPI17 and on vascular smooth muscle contraction induced by U46619 or sodium fluoride (NaF). We also investigated the effects of K⁺ channel blockers on vascular relaxation induced by GA.

Methods

Plant material

Schisandra chinensis fruits were collected from Mungyeong, Korea in September 2005. A voucher specimen (accession number *Schisandra chinensis* -PDRL-1) has been deposited in the Herbarium of Pusan National University (Park et al. 2009a). *Schisandra chinensis* was identified by our group (Professor Young Whan Choi).

Isolation of GA

The dried fruits of *Schisandra chinensis* (2.0 kg) were ground to a fine powder and were extracted three times with n-hexane in the sonicator. The suspension was filtered, evaporated under reduced pressure at low temperature and lyophilized. The brown, oily residue of hexane extract (308 g) was obtained. The remnant was extracted again with chloroform and methanol sequentially to yield chloroform (14 g) and methanol extract fractions (1368 g). The hexane extract (15.2 g) was evaporated in vacuo and chromatographed on a silica gel (40 m, J.T. Baker, NJ, USA) column (70 cm×8.0 cm) with a step gradient 0%, 5%, 10%, 20%, 30% ethyl acetate in hexane (each 1 L). The fraction 21 (800 mL, 600.5 mg) were separated on a silica gel column (100 cm×3.0 cm) with 5% acetone in CH₂Cl₂ to give a GA (200 mL, 308 mg). Pure GA was identified by HPLC on a Phenomenex Luna C18 column (Phenomenex, 150 mm×4.6 mm I.D.; 5 m particle size).

The chemical structure of GA was verified by liquid chromatography–mass spectrometry (LC–MS, Bruker BioApex FT mass spectrometer) and NMR analysis (Bruker DRX 400 spectrometer). Optical rotations were recorded on a JASCO DIP-370 digital polarimeter. Infrared spectra were recorded on an AATI Mattson Genesis Series FTIR while

NMR spectra (^1H , ^{13}C) were recorded in CDCl_3 on a Bruker DRX 400 spectrometer operating at 400MHz for ^1H and 100MHz for ^{13}C , running gradients and using residual solvent peaks as internal references (Ikeya et al. 1979). High resolution mass spectra were recorded on a Bruker FT mass spectrometer (Park et al. 2009a).

Drugs

The drugs and chemicals were obtained from the following sources: Sodium fluoride (NaF), 11,9 epoxymethano-prostaglandin $\text{F}_{2\alpha}$ (U46619), phorbol 12,13-dibutyrate (PDBu), charybdotoxin (CTX), apamin (Apa), glibenclamide (GB), phenylephrine and KCl from sigma chemicals (St. Louis, MO, USA). Stock solution of gomisin A, U46619, PDBu and GB were prepared in dimethylsulfoxide (DMSO). Stock solution of Apa was prepared in 0.05 M acetic acid. All other reagents were analytical grade.

Organ Bath Study

The investigation was conducted in accordance with Guide for the Care and Use of Laboratory Animals (Institutional Review Board, Kyungpook National University School of Medicine). Male Sprague-Dawley rats, weighing 320-350 g, were used. With animals under anesthesia (sodium pentobarbital 50 mg kg^{-1} i.p.), the thoracic aorta was immediately excised and immersed in an ice-cold, modified Krebs solution composed of (in mM) NaCl, 115.0; KCl, 4.7; CaCl_2 , 2.5; MgCl_2 , 1.2; NaHCO_3 , 25.0; KH_2PO_4 , 1.2; and dextrose, 10.0. The aorta was cleaned of all adherent connective tissue on wet filter paper, soaked in the Krebs-bicarbonate solution and cut into four ring segments (4 mm in length) as described by Seok's method (Seok et al. 2006). In order to investigate the direct effect of GA in vascular smooth

muscle, the rings were denuded of endothelium by gently rubbing the internal surface with a forcep edge. Two stainless-steel triangles were inserted through each vessel ring. Each aortic ring was suspended in a water-jacketed organ bath (22 ml) maintained at 37°C and aerated with a mixture of 95% O₂ and 5% CO₂. One triangle was anchored to a stationary support, and the other was connected to an isometric force transducer (Grass FT03C, Quincy, Mass., USA). The rings were stretched passively by imposing the optimal resting tension, 2.0 g, which was maintained throughout the experiment. Each ring was equilibrated in the organ bath solution for 90 min before the experiment involving the contractile response to 50 mM of KCl addition. Isometric contractions were recorded using a computerized data acquisition system (PowerLab/8SP, ADInstruments, Castle Hill, NSW, Australia). To determine the effect of GA on NaF, U46619 or PDBu, NaF, U46619 or PDBu were each added into organ baths to elicit tension 30 min after pretreatment with GA (0.1 mM, 0.3 mM or 1.0 mM) or vehicle. The contractile responses to 8.0 mM NaF, 30 nM U46619 and 0.1 μM PDBu were recorded for 40 min, 15 min and 40 min, respectively. To determine the effect of K⁺ channel blockers, K⁺ channel blockers were pretreated before vascular relaxation were induced by GA. GA or vehicle were added cumulatively to elicit relaxation when vascular contraction induced by phenylephrine (0.1 μM, 15 min), NaF (8.0 mM, 40 min) or U46619 (30 nM, 15 min) reached plateaus in endothelium-denuded rat aortic rings pretreated with glibenclamide (GB, 10 μM), apamin (Apa, 500 nM), charybdotoxin (CTX, 10 nM) or vehicle for 20 minutes.

SDS-PAGE for MYPT1 and CPI17

After completion of the functional study, muscle strips were quickly immersed in acetone containing 10% trichloroacetic acid (TCA) and 10 mM dithiothreitol (DTT) precooled to -80°C. The aortic rings were washed in acetone containing 5 mM DTT to remove TCA, air-

dried and stored at -80°C until use. Previously stored samples were homogenized in a buffer containing 320 mM sucrose, 50 mM Tris, 1 mM EDTA, 1% Triton X-100, 1 mM DTT, and protease inhibitors leupeptin ($10\ \mu\text{g ml}^{-1}$), trypsin inhibitor ($10\ \mu\text{g ml}^{-1}$), aprotinin ($10\ \mu\text{g ml}^{-1}$), phenylmethylsulfonyl fluoride (PMSF; $100\ \mu\text{g ml}^{-1}$) and the phosphatase inhibitor sodium orthovanadate (Na_3VO_4 ; 2 mM). Protein-matched samples (Bradford assay) were electrophoresed (SDS-PAGE), transferred to nitrocellulose membranes, and subjected to an immunoblot with a p-MYPT1 antibody (1:4,000, Upstate Biotechnology, Lake Placid, NY, USA) and a p-CPI17 antibody (1:250, Santa Cruz Biotechnology, Inc) that detect phosphorylated MYPT1 and CPI17. Anti-rabbit IgG and anti-goat IgG, conjugated with horseradish peroxidase, were used as the secondary antibody (1:4,000, Sigma, St. Louis, MO, USA and 1:1,000, Santa Cruz Biotechnology, Inc). The nitrocellulose membranes were stripped of the p-MYPT1 and p-CPI17 antibody and reblotted with total MYPT1 antibody (1:4,000, BD Biosciences Pharmingen, San Diego, CA, USA) and CPI17 antibody (1:500, Upstate Biotechnology, Lake Placid, NY, USA). Anti-mouse IgG and anti-rabbit IgG conjugated with horseradish peroxidase were used as the secondary antibody (1:4,000, Sigma, St. Louis, MO, USA and 1:1,000, Upstate Biotechnology, Lake Placid, NY, USA). The bands containing p-MYPT1, p-CPI17, t-MYPT1 and t-CPI17 were visualized with enhanced chemiluminescence (ECL) on films, and then analyzed by a computer-assisted image analyzer (Labworks, version 4.5; UVP Inc., Upland, CA).

Urea-PAGE for MLC_{20} phosphorylation

Muscle strips were quick frozen by immersion in acetone containing 10% TCA and 10 mM DTT precooled to -80°C . Muscles were washed four times with acetone containing 5 mM DTT for 15 minutes each to remove TCA and were soaked 60 minutes with frequent vortex in

100 μ l of urea sample buffer containing 20 mM Tris base, 23 mM glycine (pH 8.6), 8.0 M urea, 1 M thiourea, 10 mM DTT, 10% glycerol and, 0.04% bromophenol blue. 12.5% polyacrylamide gels containing 40% glycerol were pre-electrophoresed for 30 minutes at 300 V. The running buffer consists of 20 mM Tris base/23 mM glycine (pH 8.6), 0.97 mM thioglycolate, and 0.97 mM DTT. The urea-extracted samples (12 μ l) were electrophoresed at 300 V for 6 hours, transferred to nitrocellulose membranes, and subjected to immunoblotting with a specific myosin light chain 20 antibody (1:2,000, Sigma, St. Louis, MO, USA). Anti-mouse IgM (goat), conjugated with horseradish peroxidase, was used as a secondary antibody (1:4,000, Assay design, Ann Arbor, MI, USA) (Kim et al. 2004). The bands containing myosin light chains were visualized with enhanced chemiluminescence (ECL) on films, and then analyzed by a computer-assisted image analyzer (Labworks, version 4.5; UVP Inc., Upland, CA).

Assay for RhoA activation

Muscle strips were quick frozen by liquid nitrogen, and kept at -80°C . The RhoA assay was performed as previously described (Seok et al. 2008), the procedure followed the manufacture's protocol of G-LISATM RhoA Activation Assay Biochem KitTM (Cytoskeleton Inc, Denver, CO, USA). Briefly, previously stored samples were homogenized in a lysis buffer, and were centrifuged at 13,200 rpm for 15 min at 4°C . The resultant supernatants and equal volume of ice-cold binding buffer were added into each well for which 37 μ g of proteins were loaded. The plate was shaken on a cold orbital microplate shaker (300 rpm) for 30 min at 4°C , flicked out of the solution from wells, and incubated with diluted anti-RhoA primary antibody followed by secondary antibodies on a microplate shaker (300 rpm) at room temperature for 45 min each. The plate was incubated with HRP detection reagent for

15 min at 37°C, after addition of HRP stop buffer, the absorbance was immediately recorded at 490 nm.

Statistical analysis

Data are expressed as mean \pm SEM and were analyzed by repeated measures analysis of variance (ANOVA) for tension measurement and one-way ANOVA followed by Dunnett's test for biochemical studies. P values less than 0.05 were regarded as significant.

Results

Effect of GA on vascular contraction induced by NaF, U46619 or PDBu

Thirty minutes after the pretreatment with GA or vehicle, the concentration-response relationships to NaF, U46619 or PDBu in endothelium-denuded aortic rings were obtained by means of a cumulative addition of the chemicals (Fig. 2). The tension is expressed as a percentage to initial contractions in response to 50 mM KCl. Pretreatment with GA inhibited the contractile responses to U46619 or NaF, but not to PDBu, an activator of PKC. E_{\max} and EC_{50} for the contractile responses to NaF or U46619 in vehicle and GA preconditioned rat aortic strips are shown in Table 1. GA, at 0.3 and 1.0 mM, shifted the EC_{50} (mM) of the concentration-response curve for NaF from 4.9 ± 0.03 to 5.3 ± 0.13 ($P < 0.05$) and 6.3 ± 0.49 ($P < 0.01$) and decreased the E_{\max} (% of the KCl contraction) of the concentration-response curve for NaF from 151.8 ± 2.26 to 119.7 ± 3.22 ($P < 0.01$) and 60.4 ± 5.59 ($P < 0.01$), respectively (Fig. 2a and Table 1). Furthermore, GA (0.3 and 1.0 mM) shifted the EC_{50} ($-\log M$) of the concentration-response curve for U46619 from 8.1 ± 0.07 to 7.7 ± 0.01 ($P < 0.05$) and 7.4 ± 0.05 ($P < 0.05$) and decreased the E_{\max} (% of the KCl contraction) of the concentration-response curve for U46619 from 171.6 ± 0.53 to 120.8 ± 8.11 ($P < 0.01$) and 89.9 ± 7.12 ($P < 0.01$), respectively (Fig. 2b and Table 1). GA alone did not affect basal tension (data not shown).

Effect of K^+ channel blockers on vascular relaxation induced by GA

Since opening of K^+ channels exert vascular relaxation, we investigated whether GA exerts vascular relaxation through opening of K^+ channels by using K^+ channel blockers. Although

the vehicle did not affect vascular tension induced by phenylephrine, NaF, or U46619, GA produced vascular relaxation, which was not affected by pretreatment with glibenclamide, a blocker of ATP-sensitive K⁺ channel (Fig. 3A). In summary, pretreatment with glibenclamide (GB, 10 μM), apamin (Apa, 500 nM) or charybdotoxin (CTX, 10 nM) for 20 minutes did not affect vascular relaxation induced by GA (Fig. 3).

Inhibitory effect of GA on vascular contraction and MLC₂₀ phosphorylation induced by NaF or U46619

In order to investigate whether GA relaxes vascular contraction through regulation of thick filament, we determined the level of MLC₂₀ phosphorylation. NaF and U46619 increased phosphorylation of MLC₂₀ to $40.7 \pm 4.2\%$ or $33.7 \pm 1.3\%$, respectively, in endothelium-denuded aortic rings. Treatment of rat aortic rings with 0.3 and 1.0 mM GA significantly decreased the phosphorylation level of MLC₂₀ (Fig. 4b, d) as well as vascular contraction (Fig. 4a, c) induced by NaF or U46619 in endothelium-denuded rat aortic rings.

Inhibitory effect of GA on NaF- or U46619-induced RhoA activation

In order to determine whether GA inhibits RhoA/Rho-kinase pathway, we measured the level of GTP RhoA. NaF or U46619 increased the level of GTP RhoA (2.28 ± 0.15 fold or 2.42 ± 0.17 fold) as compared with the basal level in endothelium-denuded aortic rings. As shown in Fig. 5, GA (0.3 or 1.0 mM) nearly totally suppressed ($p < 0.05$) the level of GTP RhoA induced by NaF or U46619. However, GA itself did not affect basal level of GTP RhoA (data not shown).

Inhibitory effect of GA on NaF- or U46619-induced MYPT1_{Thr855} phosphorylation

We determined the level of the phosphorylated MYPT1_{Thr855}, a Rho-kinase substrate. NaF- or U46619-stimulated MYPT1_{Thr855} phosphorylation increased significantly (2.87 ± 0.43 and 3.10 ± 0.64 , respectively) compared with the control. As shown in Fig. 6, GA (0.3 or 1.0 mM) decreased the phosphorylation level of MYPT1_{Thr855} induced by NaF (1.59 ± 0.17 and 1.04 ± 0.12 , respectively) or U46619 (1.48 ± 0.20 and 0.87 ± 0.26 , respectively).

Inhibitory effect of GA on NaF- or U46619-induced CPI17_{Thr38} phosphorylation

The phosphorylation level of CPI17_{Thr38}, another downstream effector of Rho-kinase, was measured. NaF or U46619 increased the phosphorylation level of CPI17_{Thr38} as compared with the control in endothelium-denuded rat aortic rings. GA (0.3 or 1.0 mM) decreased the phosphorylation level of CPI17_{Thr38} induced by NaF (0.41 ± 0.07 and 0.29 ± 0.08 , respectively) (Fig. 7a) or U46619 (0.62 ± 0.05 and 0.37 ± 0.08 , respectively) (Fig. 7b).

Effect of Ro31-8220 and GA on PDBu-induced contractions and CPI17_{Thr38} phosphorylation

The contractile response to 0.1 μ M PDBu in aortic rings was obtained 30 min after the pretreatment with Ro31-8220 (1.0 μ M), GA (1.0 mM) or vehicle (Fig.8a). Pretreatment with Ro31-8220, but not with GA, inhibited the vascular contractility and phosphorylation of CPI17_{Thr38} in response to PDBu (Fig. 8a and b).

Discussion

This study demonstrates that Gomisin A (GA) attenuates vascular contraction through inhibition of the RhoA/Rho-kinase signaling pathway. GA decreases the activation of RhoA and subsequent Rho-kinase dependent phosphorylation of MYPT1_{Thr855} and CPII7_{Thr38}. GA also inhibited the phosphorylation of MLC₂₀ and the contraction in denuded rat aortic rings. However, GA did not affect K⁺ channels or PKC pathway during vascular relaxation.

The small guanosine triphosphatase RhoA (GTPase RhoA) plays an important role as a molecular switch in the enhancement of Ca²⁺ sensitivity of smooth muscle contraction (Kawano et al. 2002). Activation of receptors coupled to trimeric G proteins (G_{α12,13}) leads, through the activity of guanine nucleotide exchange factors (GEFs), to the exchange of GTP for GDP on RhoA. GTP RhoA translocates to the plasma membrane, where it interacts with Rho-kinase to initiate signaling cascades. When Rho GTPase-activating proteins (RhoGAPs) catalyze hydrolysis of GTP bound to RhoA, GDP RhoA reassociates with RhoGDI (Somlyo et al. 2003). NaF activates RhoA through activation of G-proteins (Antonny et al. 1993). Furthermore, NaF binds and inhibits RhoGAPs, thereby resulting in Rho activation (Vincent et al. 1999). U46619 activates GEF upon binding to the thromboxane A₂ receptor which is coupled to G_{12/13} (Wilson et al. 2005). The present study showed that NaF and U46619 activated RhoA approximately 2.3 fold and 2.4 fold over the resting level, respectively (Fig. 5). These data are consistent with previous reports in which NaF or U46619 activated RhoA (Seok et al. 2008; Yang et al. 2009). Furthermore, GA reduced the activation of the RhoA induced by NaF or U46619 (Fig. 5). GA may suppress GTP RhoA activation, through interaction with GEFs, RhoGAPs or RhoGDI.

The activity of myosin phosphatase decreases when PKC-potentiated inhibitory protein for heterotrimeric MLCP of 17 kDa (CPII7) or myosin phosphatase target subunit 1

(MYPT1) is phosphorylated (Feng et al. 1999). MLCP is a heterotrimer consisting of a catalytic subunit PPIc δ , a 130 kDa regulatory subunit MYPT1 and a 20 kDa subunit of unknown function (Hartshorne et al. 1998). We examined the level of phosphorylated MYPT1_{Thr855}, which is an inhibitory site and is phosphorylated by the Rho-kinase. Activation of Rho-kinase by U46619 or phenylephrine, an α 1-adrenergic agonist, phosphorylates MYPT1 at Thr855, but not MYPT1 at Thr697 (Tsai et al. 2006; Wilson et al. 2005). The phosphorylation of MYPT1_{Thr697} is independent of the stimulation of G-proteins, Rho-kinase, or PKC (Kitazawa et al. 2003; Niuro et al. 2003). We observed that GA inhibited MYPT1_{Thr855} phosphorylation induced by U46619 or NaF (Fig. 6). These observations suggest that GA inhibits the phosphorylation of MYPT1_{Thr855} induced by Rho-kinase.

CPI17 is another downstream effector of Rho-kinase, which was first isolated from porcine aorta and identified as a substrate of PKC at Thr38 (Eto et al. 1995). U46619-induced CPI17_{Thr38} phosphorylation was abolished by a Rho-kinase inhibitor Y27632, suggesting that Rho-kinase is involved in U46619-induced CPI17 phosphorylation and contractions (Pang et al. 2005). These reports showed that U46619 caused CPI17 phosphorylation through activation of the RhoA/Rho-kinase pathway, whereas PDBu phosphorylates CPI17 through direct activation of protein kinase C pathway. In a separate study of our laboratory, activation of Rho-kinase by NaF, or U46619 phosphorylates CPI17_{Thr38} (Seok et al. 2008; Yang et al. 2009). Our data also showed that NaF or U46619 significantly increased CPI17_{Thr38} phosphorylation, which was inhibited by GA (Fig. 7). However, PDBu-induced CPI17_{Thr38} phosphorylation was not inhibited by GA (Fig. 8B).

It is well known that K⁺ channels play an important role in the regulation of muscle contractility and vascular tone. Because K⁺ channels are the dominant ion conductive pathway in vascular smooth muscle, inhibition of K⁺ channels lead to membrane depolarization and vascular contraction (Jackson 2000; Nelson et al. 1995; Standen et al.

1998). However, in our experiment (Fig. 3), the relaxant action of GA in the rat aorta did not seem to be due to the opening of K⁺ channels, since the vasorelaxant effects of GA were unaffected by pretreatment with glibenclamide (a blocker of ATP-sensitive K⁺ channels), apamin (a blocker of small conductance Ca²⁺-activated K⁺ channels) and charybdotoxin (a blocker of large-conductance Ca²⁺-activated K⁺ channels). These data are in accordance with previous report that vasorelaxant action of *Schisandra chinensis* extracts was unaffected by tetraethylammonium, a nonselective blocker of K⁺ channels (Park et al. 2009b). Smooth muscle contraction is mainly regulated by the level of phosphorylation of MLC₂₀, which is determined by the opposing action of myosin light chain kinase (MLCK) and MLCP. MLCK mediates MLC phosphorylation causing contraction in a Ca²⁺/calmodulin-dependent manner (Kamm et al. 1985). Conversely, MLCP mediates dephosphorylation of phosphorylated MLC causing relaxation (Bialojan et al. 1987; Somlyo et al. 1994). Furthermore, activation of Rho-kinase by NaF or U46619 inhibits the activity of MLCP through phosphorylation of regulatory MYPT1_{Thr855}, leading to an increased MLC₂₀ phosphorylation and contraction (Wang et al. 2001; Wilson et al. 2005; Yang et al. 2009). In the present study, GA reduced not only vascular contraction but also the phosphorylation of MLC₂₀ induced by NaF or U46619 in endothelium-denuded rat aortic rings (Fig. 4). GA inhibited concentration-response curves to U46619 and to NaF in endothelium-denuded aortic rings. This result is in accordance with the finding that GA decreased vascular contraction and MLC₂₀ phosphorylation induced by phenylephrine and that ML 9, an inhibitor of MLCK, failed to modify GA-induced relaxation. These data suggest that the vasorelaxation by GA is mediated by dephosphorylation of phosphorylated MLC through activation of MLCP (Park et al. 2007).

A dozen of years ago, the Rho-kinase was identified to be involved in development of high blood pressure (Uehata et al. 1997). Rho kinase has been identified as an important target for treatment of several cardiovascular diseases (Budzyn et al. 2006; Lohn et al. 2009).

GA decreased vascular contraction induced by NaF or U46619 through inhibition of the RhoA/Rho-kinase pathway. Therefore, GA may be a potential lead for development of therapeutic drugs. Although GA induces not only endothelium-dependent but also endothelium-independent vascular relaxation in isolated thoracic aorta (Park et al. 2007; Rhyu et al. 2006), GA may have a main action through activation of nitric oxide (NO) pathway in endothelium. However, in some instances such as endothelial dysfunction, it may exert endothelium-independent vascular relaxation through activation of activation of RhoA/Rho-kinase signaling pathway which inhibits MLC phosphatase.

In conclusion, GA directly relaxes NaF- and U46619-, but not PDBu-, induced vascular contraction in the absence of endothelium. These results suggest that GA attenuates vascular contractions through the inhibition of the RhoA/Rho-kinase pathway. However, K⁺ channels are not involved in the vascular relaxation induced by GA.

References

- Antonny B, Sukumar M, Bigay J, Chabre M, Higashijima T (1993) The mechanism of aluminum-independent G-protein activation by fluoride and magnesium. ³¹P NMR spectroscopy and fluorescence kinetic studies. *J Biol Chem* 268:2393-402
- Bialojan C, Ruegg JC, DiSalvo J (1987) A myosin phosphatase modulates contractility in skinned smooth muscle. *Pflugers Arch* 410:304-12
- Budzyn K, Marley PD, Sobey CG (2006) Targeting Rho and Rho-kinase in the treatment of cardiovascular disease. *Trends Pharmacol Sci* 27:97-104
- Budzyn K, Sobey CG (2007) Vascular rho kinases and their potential therapeutic applications. *Curr Opin Drug Discov Devel* 10:590-6
- Chen DF, Zhang SX, Xie L, Xie JX, Chen K, Kashiwada Y, Zhou BN, Wang P, Cosentino LM, Lee KH (1997) Anti-AIDS agents--XXVI. Structure-activity correlations of gomisins-G-related anti-HIV lignans from *Kadsura interior* and of related synthetic analogues. *Bioorg Med Chem* 5:1715-23
- Chiu PY, Mak DH, Poon MK, Ko KM (2002) In vivo antioxidant action of a lignan-enriched extract of *Schisandra* fruit and an anthraquinone-containing extract of *Polygonum* root in comparison with schisandrin B and emodin. *Planta Med* 68:951-6
- Choi YW, Takamatsu S, Khan SI, Srinivas PV, Ferreira D, Zhao J, Khan IA (2006) Schisandrene, a dibenzocyclooctadiene lignan from *Schisandra chinensis*: structure-antioxidant activity relationships of dibenzocyclooctadiene lignans. *J Nat Prod* 69:356-9
- Eto M, Ohmori T, Suzuki M, Furuya K, Morita F (1995) A novel protein phosphatase-1 inhibitory protein potentiated by protein kinase C. Isolation from porcine aorta media and characterization. *J Biochem* 118:1104-7
- Feng J, Ito M, Kureishi Y, Ichikawa K, Amano M, Isaka N, Okawa K, Iwamatsu A, Kaibuchi K, Hartshorne DJ, Nakano T (1999) Rho-associated kinase of chicken gizzard smooth muscle. *J Biol Chem* 274:3744-52

Hartshorne DJ, Ito M, Erdodi F (1998) Myosin light chain phosphatase: subunit composition, interactions and regulation. *J Muscle Res Cell Motil* 19:325-41

He XG, Lian LZ, Lin LZ (1997) Analysis of lignan constituents from *Schisandra chinensis* by liquid chromatography-electrospray mass spectrometry. *J Chromatogr A* 757:81-7

Hirata K, Kikuchi A, Sasaki T, Kuroda S, Kaibuchi K, Matsuura Y, Seki H, Saida K, Takai Y (1992) Involvement of rho p21 in the GTP-enhanced calcium ion sensitivity of smooth muscle contraction. *J Biol Chem* 267:8719-22

Hirooka Y, Shimokawa H, Takeshita A (2004) Rho-kinase, a potential therapeutic target for the treatment of hypertension. *Drug News Perspect* 17:523-7

Ikeya Y, Taguchi H, Yosioka I, Iitaka Y, Kobayashi H (1979) The constituents of *Schizandra chinensis* Baill. II. The structure of a new lignan, gomisin D. *Chem Pharm Bull (Tokyo)* 27: 1395-401.

Jackson WF (2000). Ion channels and vascular tone. *Hypertension* 35:173-8

Kamm KE, Stull JT (1985) The function of myosin and myosin light chain kinase phosphorylation in smooth muscle. *Annu Rev Pharmacol Toxicol* 25:593-620

Kawano Y, Yoshimura T, Kaibuchi K (2002) Smooth muscle contraction by small GTPase Rho. *Nagoya J Med Sci* 65:1-8

Kim IK, Park TG, Kim YH, Cho JW, Kang BS, Kim CY (2004) Heat-shock response is associated with enhanced contractility of vascular smooth muscle in isolated rat aorta. *Naunyn Schmiedeberg Arch Pharmacol* 369:402-7

Kitazawa T, Eto M, Woodsome TP, Khalequzzaman M (2003) Phosphorylation of the myosin phosphatase targeting subunit and CPI-17 during Ca²⁺ sensitization in rabbit smooth muscle. *J Physiol* 546:879-89

Leung T, Manser E, Tan L, Lim L (1995) A novel serine/threonine kinase binding the Ras-related RhoA GTPase which translocates the kinase to peripheral membranes. *J Biol Chem* 270:29051-4

Lohn M, Plettenburg O, Ivashchenko Y, Kannt A, Hofmeister A, Kadereit D, Schaefer M, Linz W, Kohlmann M, Herbert JM, Janiak P, O'Connor SE, Ruetten H (2009) Pharmacological characterization of SAR407899, a novel rho-kinase inhibitor. *Hypertension* 54:676-83

Nakajima K, Taguchi H, Ikeya Y, Endo T, Yosioka I (1983) Constituents of *Schizandra chinensis* Baill. XIII. Quantitative analysis of lignans in the fruits of *Schizandra chinensis* Baill. by high performance liquid chromatography. *Yakugaku Zasshi* 103:743-9

Nelson MT, Quayle JM (1995) Physiological roles and properties of potassium channels in arterial smooth muscle. *Am J Physiol* 268:C799-822

Niuro N, Koga Y, Ikebe M (2003) Agonist-induced changes in the phosphorylation of the myosin-binding subunit of myosin light chain phosphatase and CPI17, two regulatory factors of myosin lightchain phosphatase, in smooth muscle. *Biochem J* 369:117-28

Pang H, Guo Z, Su W, Xie Z, Eto M, Gong MC (2005) RhoA-Rho kinase pathway mediates thrombin- and U-46619-induced phosphorylation of a myosin phosphatase inhibitor, CPI-17, in vascular smooth muscle cells. *Am J Physiol Cell Physiol* 289:C352-60

Park JY, Lee SJ, Yun MR, Seo KW, Bae SS, Park JW, Lee YJ, Shin WJ, Choi YW, Kim CD (2007) Gomisins A from *Schizandra chinensis* induces endothelium-dependent and direct relaxation in rat thoracic aorta. *Planta Med* 73:1537-42

Park JY, Shin HK, Choi YW, Lee YJ, Bae SS, Han J, Kim CD (2009a) Gomisins A induces Ca²⁺-dependent activation of eNOS in human coronary artery endothelial cells. *J Ethnopharmacol* 125:291-6

Park JY, Shin HK, Lee YJ, Choi YW, Bae SS, Kim CD (2009b) The mechanism of vasorelaxation induced by *Schizandra chinensis* extract in rat thoracic aorta. *J Ethnopharmacol* 121:69-73

Rhyu MR, Kim EY, Yoon BK, Lee YJ, Chen SN (2006) Aqueous extract of *Schizandra chinensis* fruit causes endothelium-dependent and -independent relaxation of isolated rat thoracic aorta. *Phytomedicine* 13:651-7

Seok Y, Kim JI, Ito M, Kureishi Y, Nakano T, Kim SO, Lim DG, Park WH, Kim I (2006) Heat shock-induced augmentation of vascular contractility is independent of rho-kinase. *Clin Exp Pharmacol Physiol* 33:264-8

Seok YM, Baek I, Kim YH, Jeong YS, Lee IJ, Shin DH, Hwang YH, Kim IK (2008) Isoflavone attenuates vascular contraction through inhibition of the RhoA/Rho-kinase signaling pathway. *J Pharmacol Exp Ther* 326:991-8

Shimokawa H, Takeshita A (2005) Rho-kinase is an important therapeutic target in cardiovascular medicine. *Arterioscler Thromb Vasc Biol* 25:1767-75

Somlyo AP, Somlyo AV (2003) Ca²⁺ sensitivity of smooth muscle and nonmuscle myosin II: modulated by G proteins, kinases, and myosin phosphatase. *Physiol Rev* 83:1325-58

Somlyo AP, Somlyo AV (1994) Signal transduction and regulation in smooth muscle. *Nature* 372:231-6

Standen NB, Quayle JM (1998) K⁺ channel modulation in arterial smooth muscle. *Acta Physiol Scand* 164:549-57

Tsai, MH, Jiang, MJ (2006) Rho-kinase-mediated regulation of receptor-agonist-stimulated smooth muscle contraction. *Pflugers Arch* 453:223-32

Uehata M, Ishizaki T, Satoh H, Ono T, Kawahara T, Morishita T, Tamakawa H, Yamagami K, Inui J, Maekawa M, Narumiya S (1997) Calcium sensitization of smooth muscle mediated by a Rho-associated protein kinase in hypertension. *Nature* 389:990-4

Vincent S, Settleman J (1999) Inhibition of RhoGAP activity is sufficient for the induction of Rho-mediated actin reorganization. *European Cell Biology* 78:539-548

Wang P, Verin AD, Birukova A, Gilbert-McClain LI, Jacobs K, Garcia JG (2001) Mechanisms of sodium fluoride-induced endothelial cell barrier dysfunction: role of MLC phosphorylation. *Am J Physiol Lung Cell Mol Physiol* 281:L1472-83

Wilson DP, Susnjar M, Kiss E, Sutherland C, Walsh MP (2005) Thromboxane A₂-induced contraction of rat caudal arterial smooth muscle involves activation of Ca²⁺ entry and Ca²⁺ sensitization: Rho-associated kinase-mediated phosphorylation of MYPT1 at Thr-855, but not Thr-697. *Biochem J* 389:763-74

Wirth A, Benyo Z, Lukasova M, Leutgeb B, Wettschureck N, Gorbey S, Orsy P, Horvath B, Maser-Gluth C, Greiner E, Lemmer B, Schutz G, Gutkind JS, Offermanns S (2008) G12-G13-LARG-

mediated signaling in vascular smooth muscle is required for salt-induced hypertension. *Nat Med* 14:64-8

Wu MD, Huang RL, Kuo LM, Hung CC, Ong CW, Kuo YH (2003) The anti-HBsAg (human type B hepatitis, surface antigen) and anti-HBeAg (human type B hepatitis, e antigen) C18

dibenzocyclooctadiene lignans from *Kadsura matsudai* and *Schizandra arisanensis*. *Chem Pharm Bull (Tokyo)* 51:1233-6

Yang E, Jeon SB, Baek I, Chen ZA, Jin Z, Kim IK (2009) 17beta-estradiol attenuates vascular contraction through inhibition of RhoA/Rho kinase pathway. *Naunyn Schmiedebergs Arch Pharmacol* 380:35-44

Yasukawa K, Ikeya Y, Mitsuhashi H, Iwasaki M, Aburada M, Nakagawa S, Takeuchi M, Takido M (1992) Gomisin A inhibits tumor promotion by 12-O-tetradecanoylphorbol-13-acetate in two-stage carcinogenesis in mouse skin. *Oncology* 49:68-71

Table 1. Maximum contraction (E_{\max}) and EC_{50} values for the contractile responses to NaF or U46619 during pretreatment with GA.

| GA (mM) | NaF | | U46619 | |
|----------------|--------------------|----------------|--------------------|--------------------|
| | E_{\max} (% KCl) | EC_{50} (mM) | E_{\max} (% KCl) | EC_{50} (-log M) |
| Vehicle | 151.8 ± 2.26 | 4.9 ± 0.03 | 171.6 ± 0.53 | 8.1 ± 0.07 |
| 0.1 | 153.0 ± 2.67 | 5.0 ± 0.09 | 171.6 ± 7.73 | 8.0 ± 0.01 |
| 0.3 | 119.7 ± 3.22** | 5.3 ± 0.13* | 120.8 ± 8.11** | 7.7 ± 0.01* |
| 1.0 | 60.4 ± 5.59** | 6.3 ± 0.49** | 89.9 ± 7.12** | 7.7 ± 0.01* |

Data are expressed as means of four experiments, with vertical bars showing SEM. * $P < 0.05$,

** $P < 0.01$ vs. NaF or U46619 alone.

Fig. 1. Chemical structure of gomisin A.

Fig. 2. Effect of gomisin A (GA) on NaF (A)-, U46619 (B)- or PDBu (C)-induced contractions. NaF, U46619 or PDBu were each added cumulatively to elicit tension 30 min after pretreatment with GA or vehicle (DMSO) in denuded rat aortic rings. Developed tension is expressed as a percentage of the maximal contraction to 50 mM KCl. Data are expressed as means of four experiments with vertical bars showing SEM. ** $P < 0.01$ vs. vehicle.

Fig. 3. Effect of K^+ channel blockers pretreatment on vascular relaxation induced by GA. GA (0.1, 0.3 or 1.0 mM) or vehicle were added cumulatively to elicit relaxation when vascular contraction induced by phenylephrine (0.1 μ M), NaF (8.0 mM) or U46619 (30 nM) reached plateaus in endothelium-denuded rat aortic rings pretreated with vehicle, glibenclamide (GB), a blocker of ATP-sensitive K^+ channel (10 μ M), apamin (Apa), a blocker of small conductance Ca^{2+} -activated K^+ channel (500 nM), charybdotoxin (CTX), a blocker of large-conductance Ca^{2+} -activated K^+ channel (10 nM), for 20 minutes. (A) Representative traces show relaxing responses to GA. Developed tension is expressed as a percentage of the maximal contraction to phenylephrine (B), NaF (C) or U46619 (D). Data are expressed as the means of four experiments with vertical bars showing SEM.

Fig. 4. Inhibitory effect of GA on NaF- or U46619-induced MLC_{20} phosphorylation in rat aorta. NaF (8.0 mM) (A) or U46619 (30 nM) (C) were each added to elicit tension 30 min after pretreatment with GA (0.3 or 1.0 mM) or vehicle to denuded aortic rings.

Developed tension is expressed as a percentage of the maximum contractions to 50 mM KCl. (6 aortic rings). When the tension reached plateaus, the phosphorylation level of MLC₂₀ in response to NaF (B) or U46619 (D) was measured and was expressed as a percentage of the total MLC₂₀ (4 aortic rings). Data are expressed as means with vertical bars showing SEM. ** P < 0.01 vs. vehicle (A and C). ## P < 0.01 vs. control. ** P < 0.01 vs. NaF or U46619 alone (B and D).

Fig. 5. Inhibitory effect of GA on NaF (A)- or U46619 (B)-induced RhoA activation in rat aorta. NaF (6.0 mM) or U46619 (30 nM) were each added to elicit tension 30 min after pretreatment with GA (0.3 or 1.0 mM) or vehicle to denuded aortic rings. The amount of GTP-RhoA was assayed by a RhoA G-LISATM Activation Assay kit. Absorbance of the control (OD₄₉₀ of around 0.4) was expressed as 1 arbitrary unit. Data are expressed as means of four experiments, with vertical bars showing SEM. ## P < 0.01 vs. control. * P < 0.05, ** P < 0.01 vs. NaF or U46619 alone.

Fig. 6. Inhibitory effect of GA on phosphorylation level of MYPT1_{Thr855} induced by NaF (A) or U46619 (B). NaF (8.0 mM) or U46619 (30 nM) were each added to elicit tension 30 min after pretreatment with GA (0.3 or 1.0 mM) or vehicle to denuded aortic rings. MYPT1 phosphorylation at Thr855 was assessed by western blot. Upper and lower bands in representative western blots were probed with anti-pMYPT1 and anti-tMYPT1 antibodies, respectively. The ratio of density of phosphorylated MYPT1 (upper) to that of the total MYPT1 (lower) regarding the control was expressed as 1 arbitrary unit. Data are expressed as the means of four experiments, with vertical bars showing SEM. ## P < 0.01 vs. control. * P < 0.05, ** P < 0.01 vs. NaF or U46619 alone.

Fig. 7. Inhibitory effect of GA on phosphorylation of CPI17_{Thr38} induced by NaF (A) or U46619 (B). NaF (8.0 mM) or U46619 (30 nM) were each tension 30 min after pretreatment with GA (0.3 or 1.0 mM) or vehicle to denuded aortic rings. CPI17 phosphorylation at Thr38 was assessed by western blot. Upper and lower bands in representative western blots were probed with anti-pCPI17 and anti-tCPI17 antibodies, respectively. The ratio of density of phosphorylated CPI17 (upper) to that of the total CPI17 (lower) regarding the positive control was expressed as 1 arbitrary unit. Data are expressed as means of four experiments with vertical bars showing SEM. ^{##} P < 0.01 vs. control. ^{**} P < 0.01 vs. NaF or U46619 alone.

Fig. 8. Effect of PKC inhibitor Ro31-8220, or gomisin A on PDBu-induced contraction and CPI17 phosphorylation in rat aorta. PDBu (0.1 μM) was added to elicit tension 30 min after pretreatment with Ro31-8220 (1.0 μM), gomisin A (1.0 mM), or vehicle to denuded aortic rings. (A) Developed tension is expressed as a percentage of the maximum contractions to 50 mM KCl (4 aortic rings). (B) CPI17 phosphorylation at Thr38 was assessed by means of western blot after PDBu treatment. Upper, middle and lower bands in representative western blots were probed with anti-pCPI17, anti-tCPI17 and anti-β-actin antibodies, respectively. The ratio of density of phosphorylated CPI17 (upper) to that of total CPI17 (middle) for treatment with PDBu was expressed as 1 arbitrary unit. Data are expressed as means of four experiments with vertical bars showing SEM. ^{**} P < 0.01 vs. vehicle (A). ^{##} P < 0.01 vs. control. ^{**} P < 0.01 vs. PDBu alone (B).

Fig. 1.

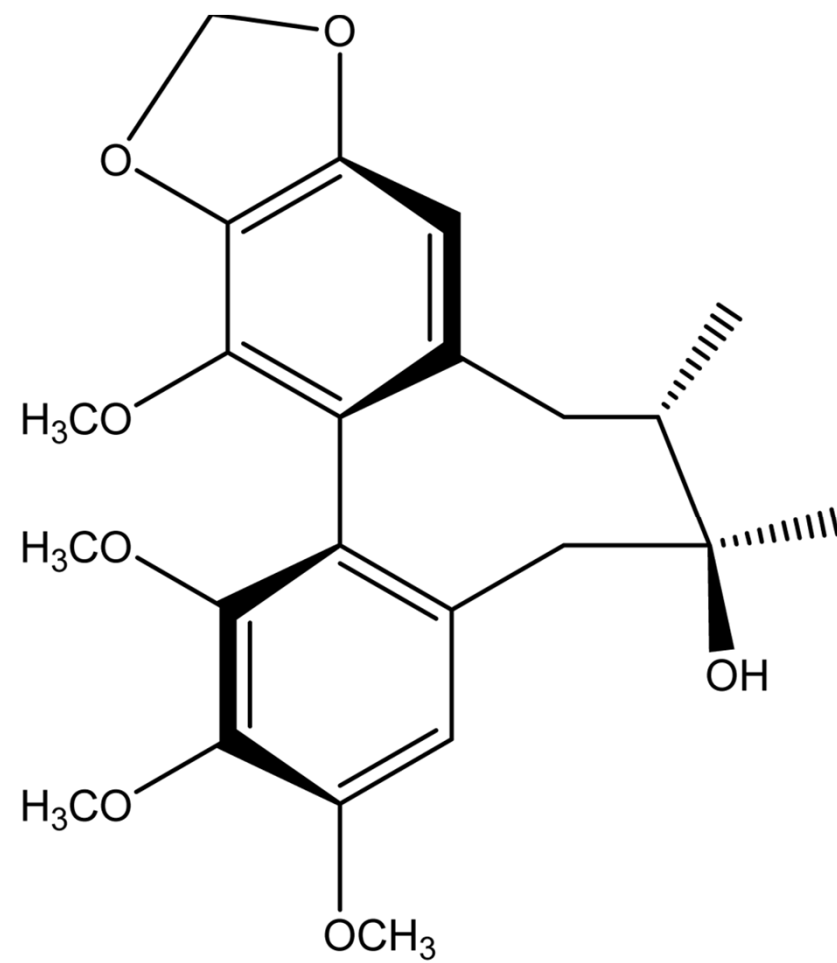


Fig. 2.

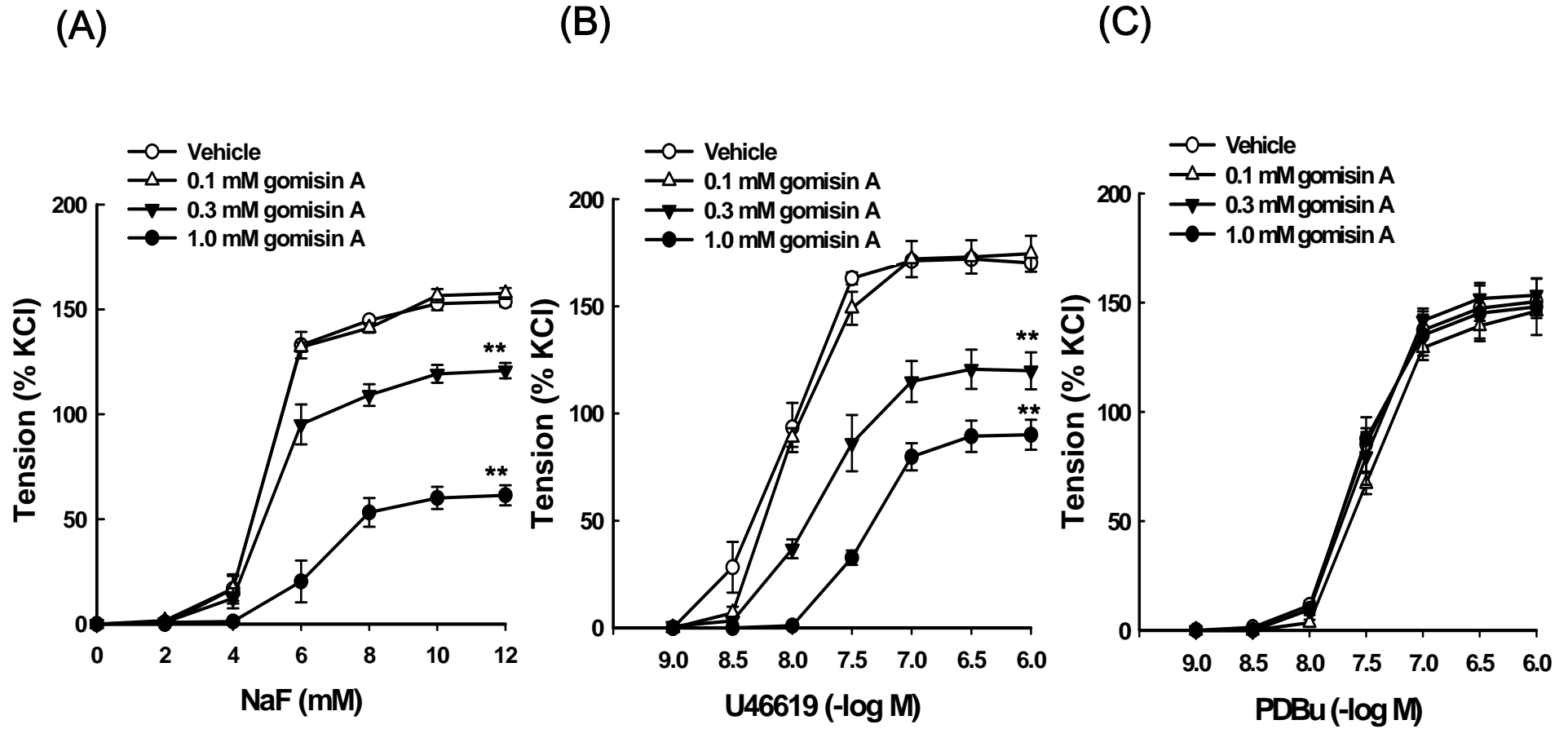


Fig. 3.

(A)

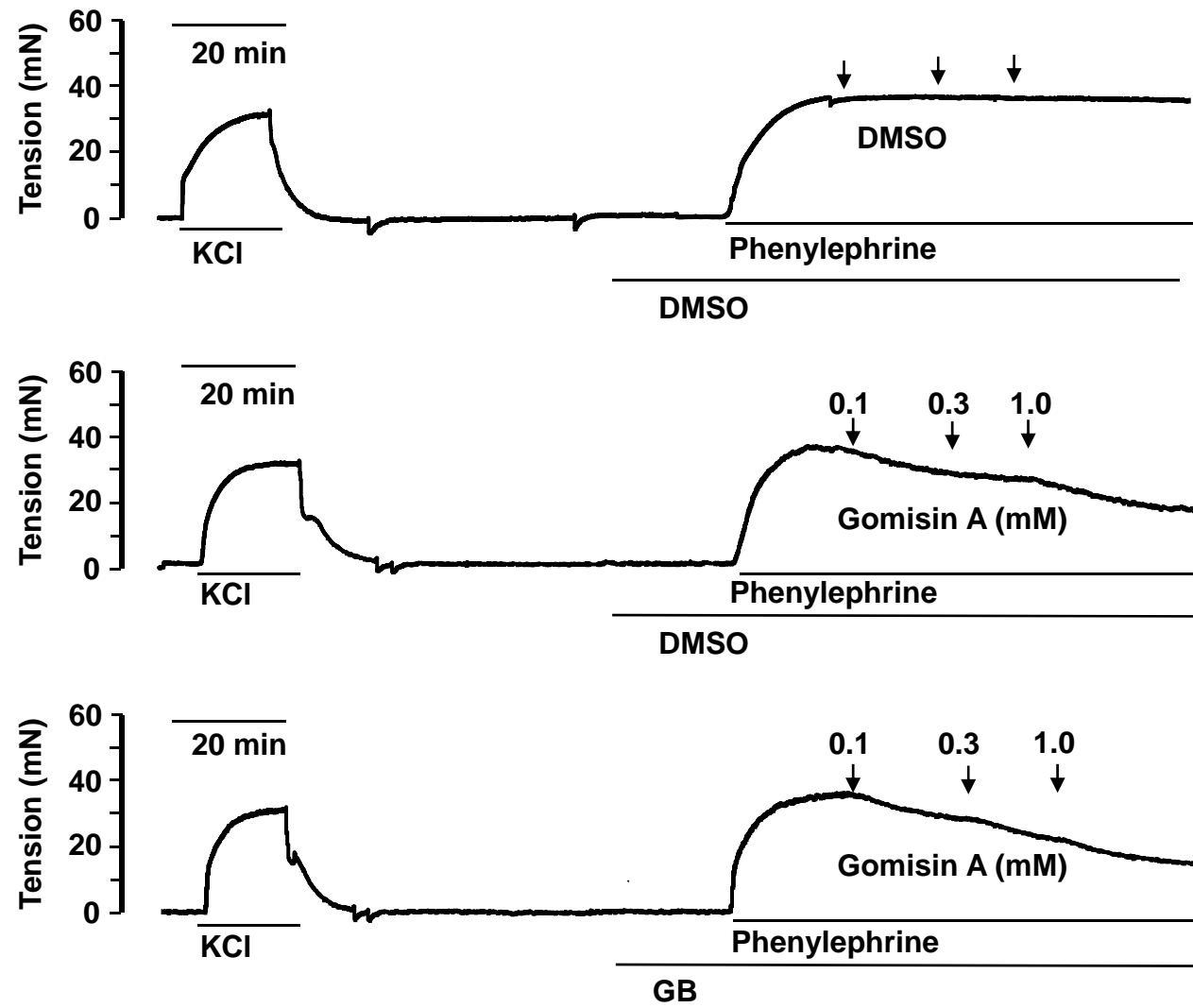
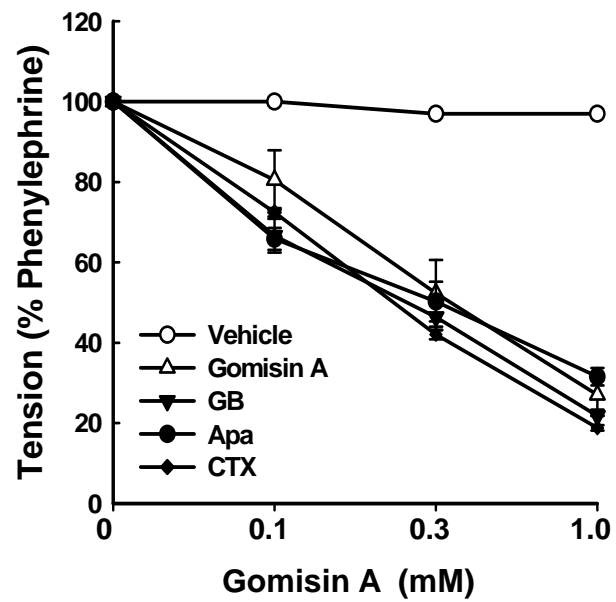
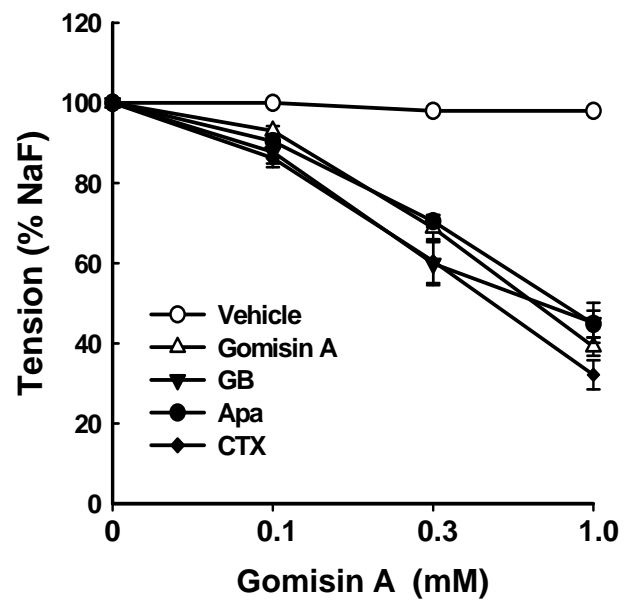


Fig. 3.

(B)



(C)



(D)

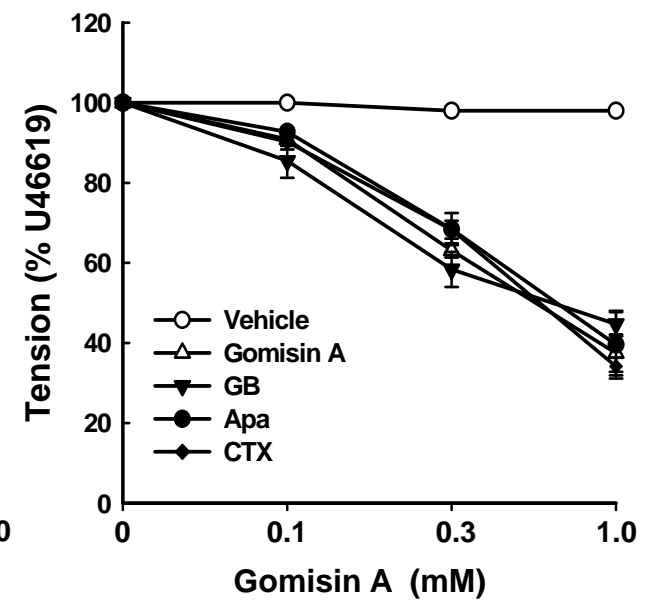


Fig. 4.

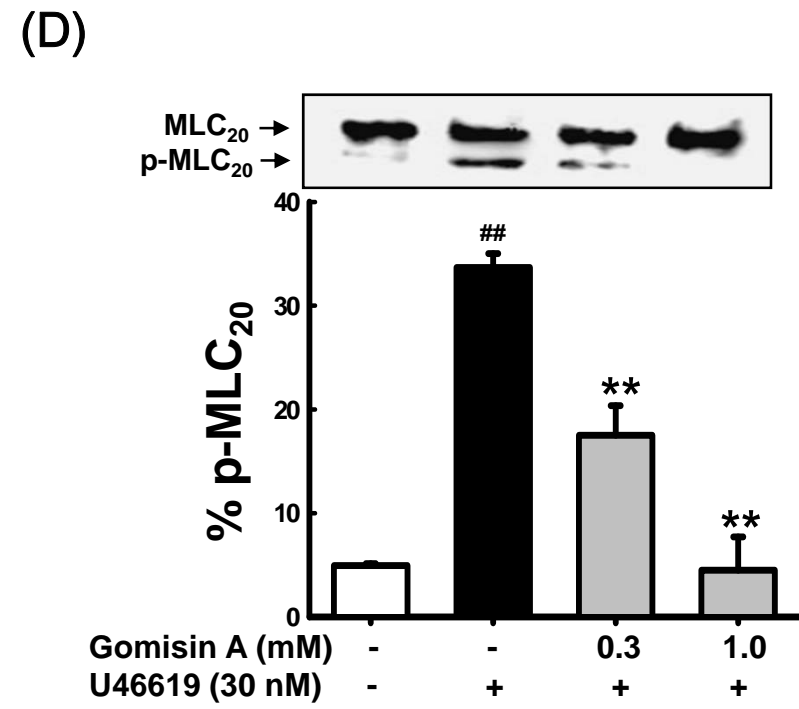
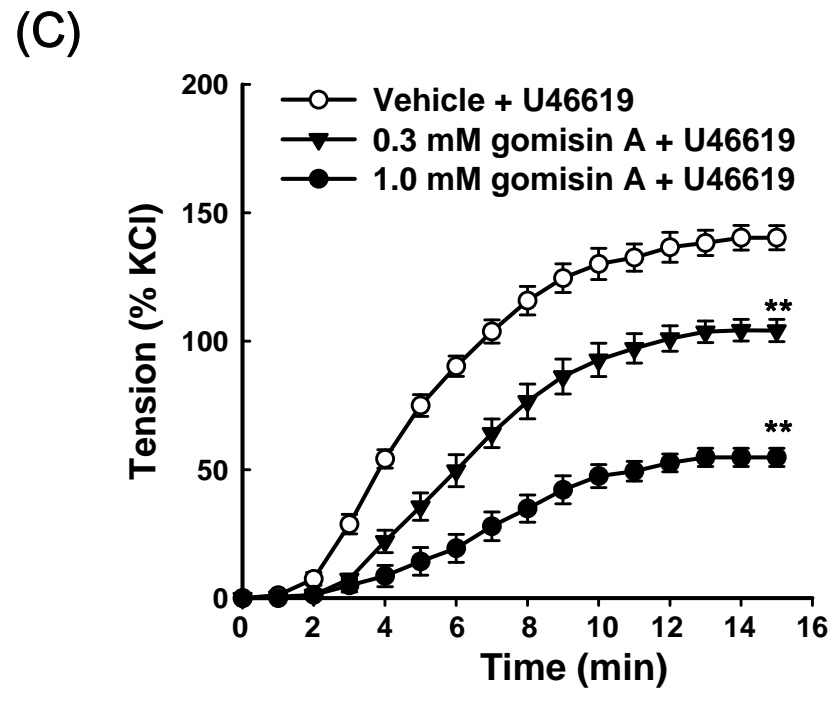
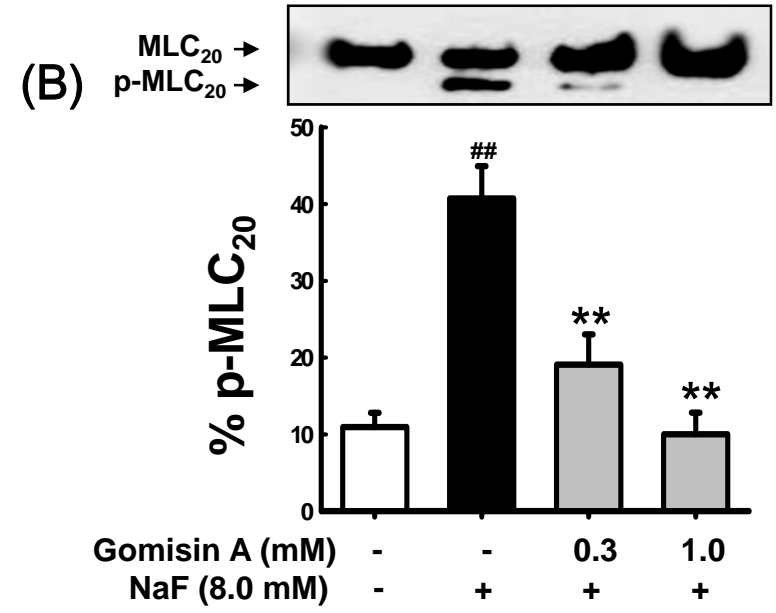
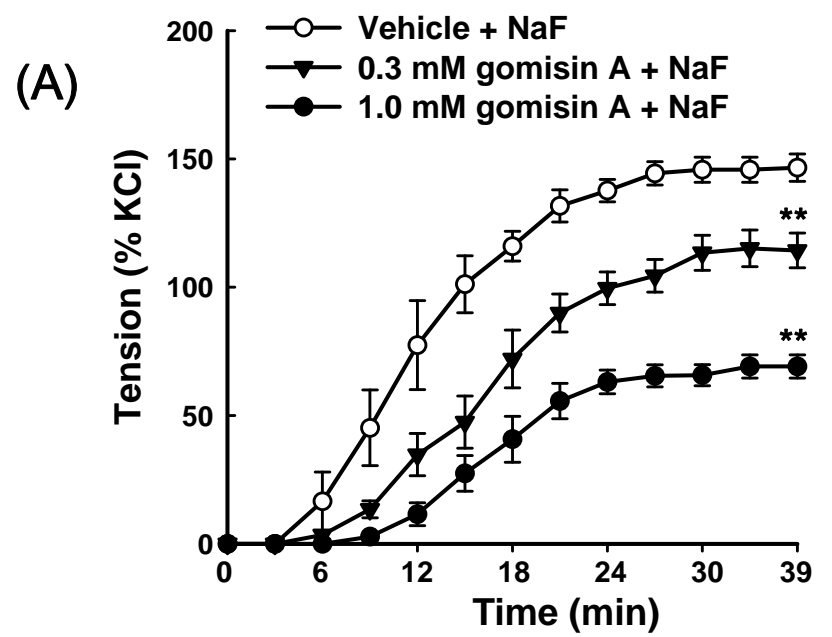
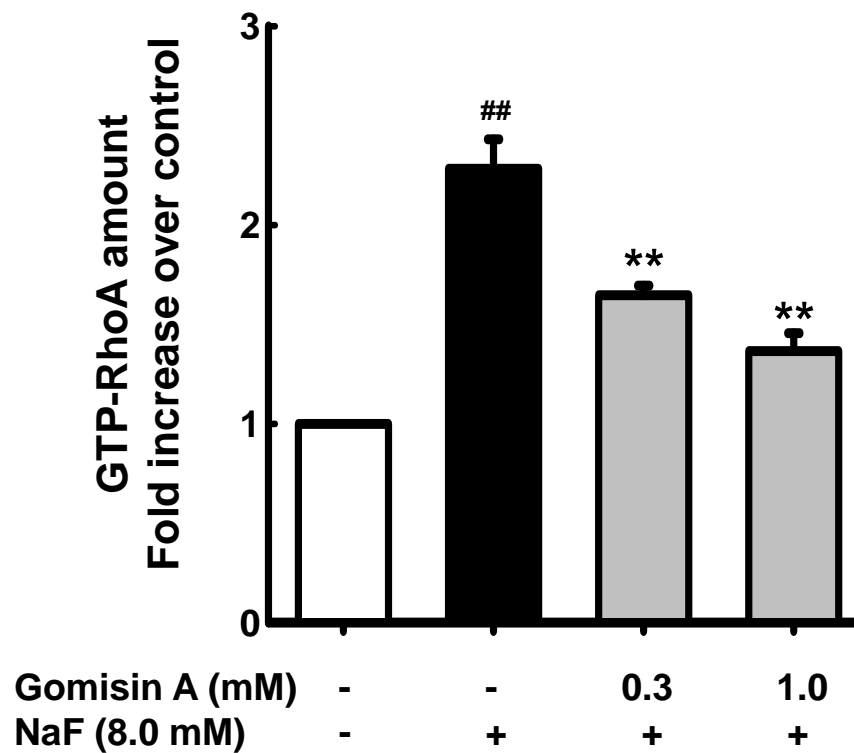


Fig. 5.

(A)



(B)

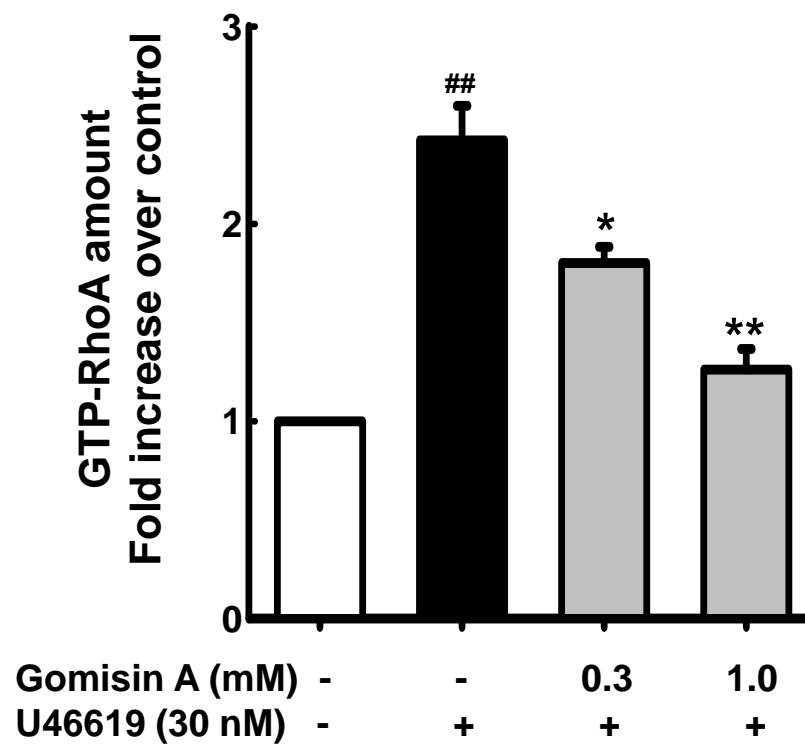
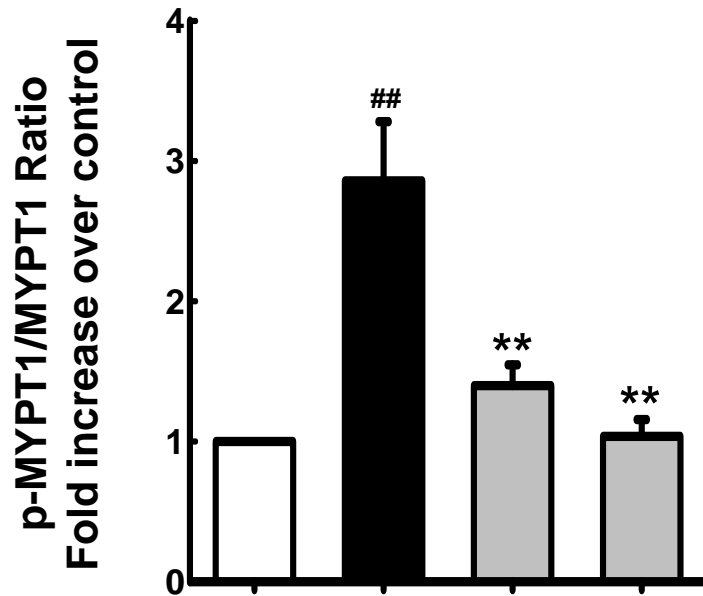
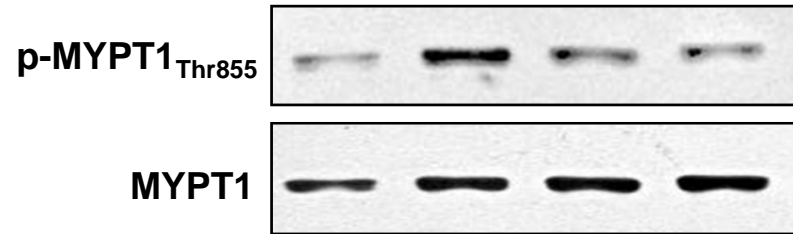


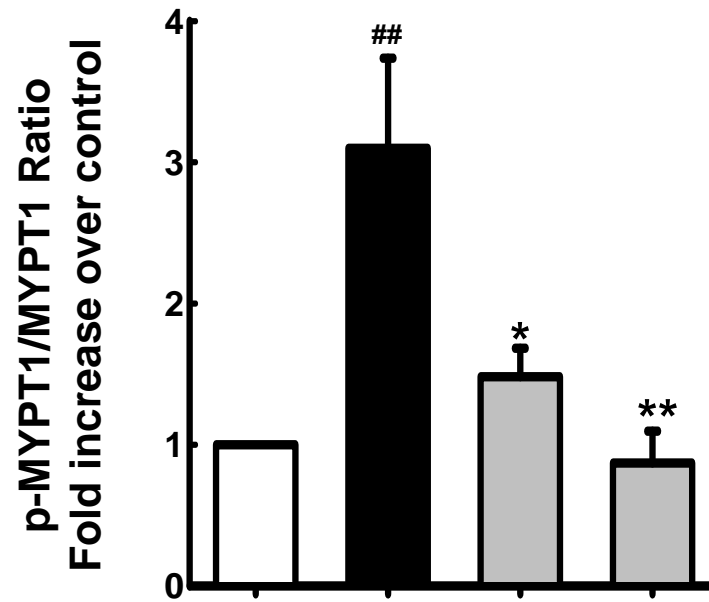
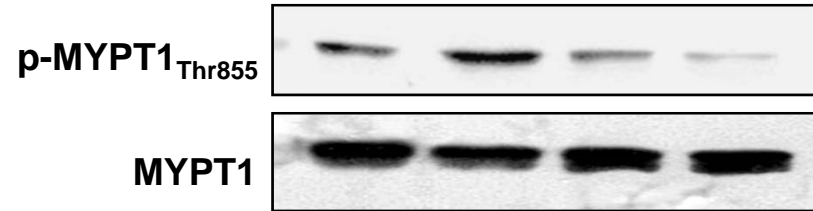
Fig. 6.

(A)



Gomisin A (mM) - - 0.3 1.0
NaF (8.0 mM) - + + +

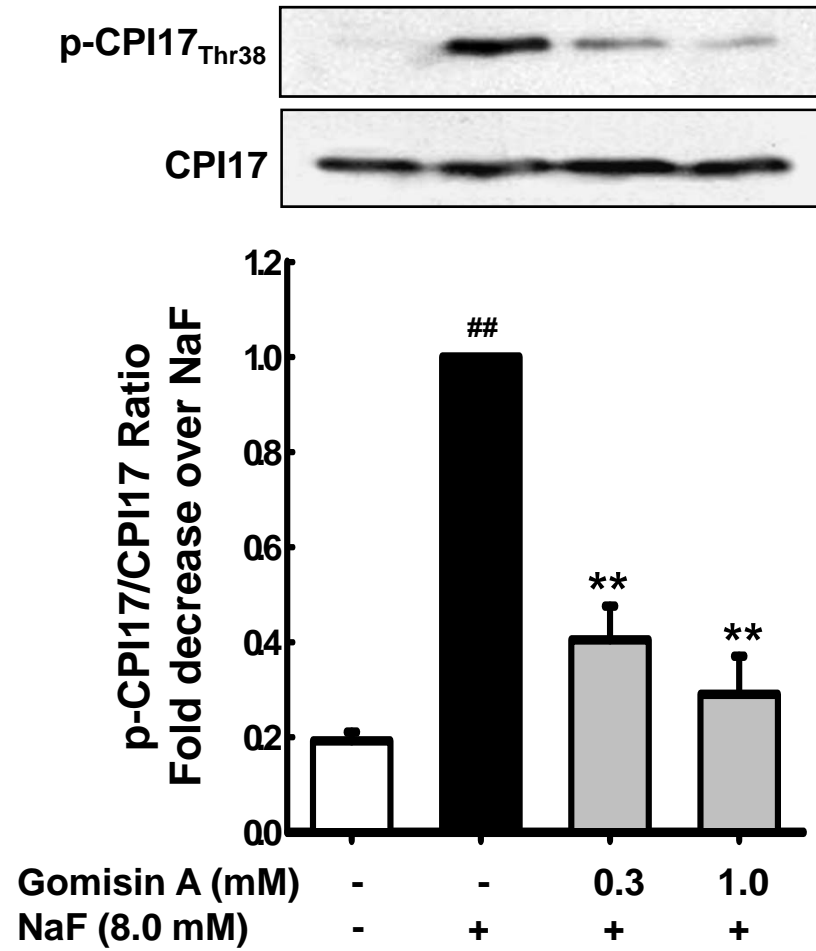
(B)



Gomisin A (mM) - - 0.3 1.0
U46619 (30 nM) - + + +

Fig. 7.

(A)



(B)

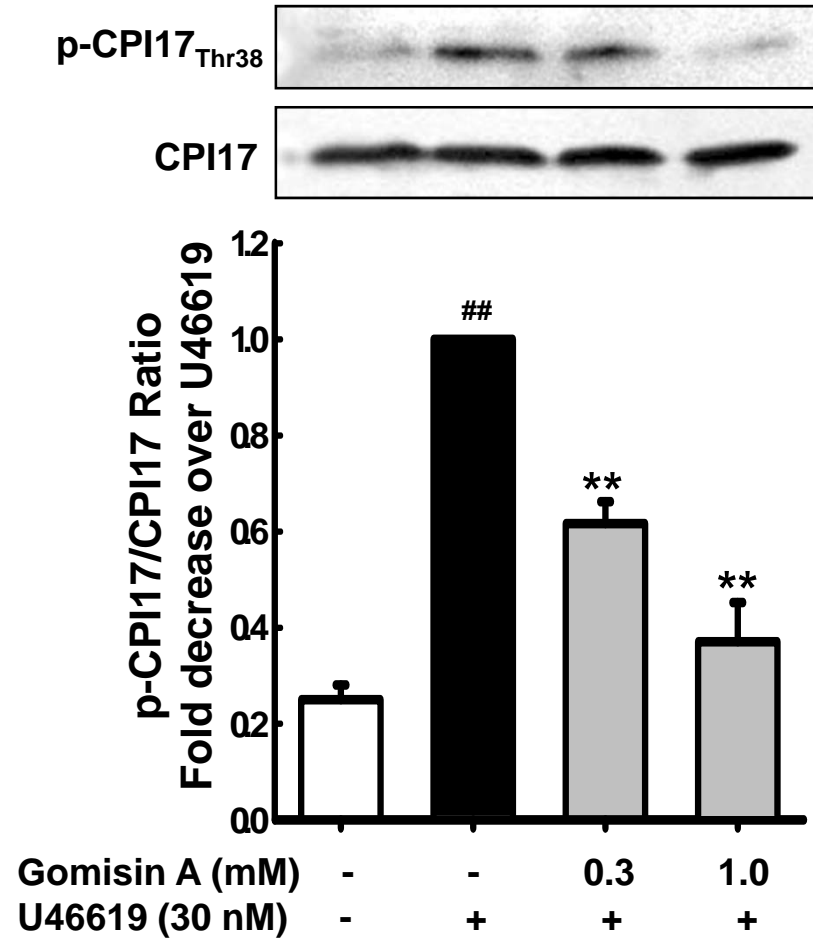
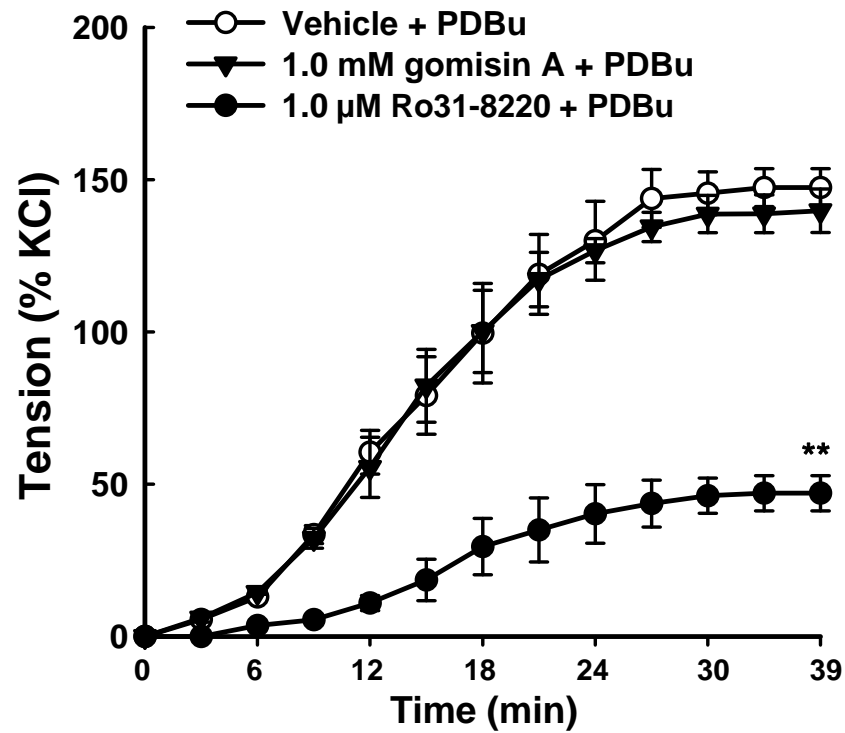
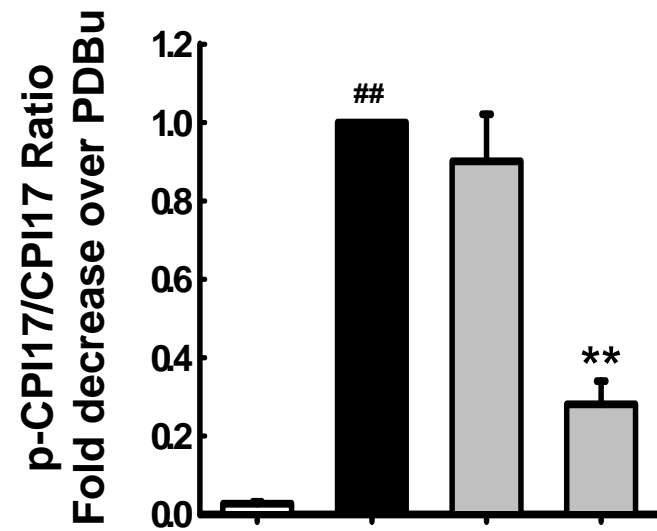
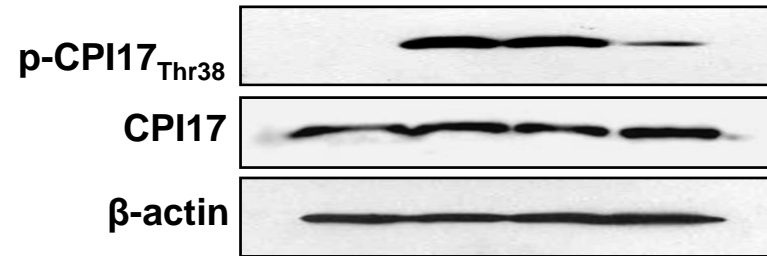


Fig. 8.

(A)



(B)



| | | | | |
|--------------------|---|---|---|---|
| Gomisin A (1.0 mM) | - | - | + | - |
| Ro31-8220 (1.0 μM) | - | - | - | + |
| PDBu (0.1 μM) | - | + | + | + |